9

Assessment of Coronary Artery Bypass Graft (CABG) Patency and Graft Disease Using Multidetector Computed Tomography (MDCT)

Bong Gun Song et al.*
Cardiovascular imaging center, Cardiac and Vascular Center
Sungkyunkwan University Samsung Changwon Hospital
Inje University Ilsan Paik Hospital
Konkuk University Hospital
Republic of Korea

1. Introduction

Coronary artery bypass graft (CABG) surgery is the standard care in the treatment of advanced coronary artery disease. Notwithstanding the clear benefits of bypass grafting, recurrent chest pain after myocardial revascularization surgery is a common postoperative presentation and the long-term clinical outcome after myocardial revascularization surgery is largely dependent on graft patency and the progression of coronary artery disease. Therefore, assessment of the status of the grafts and graft disease after CABG surgery is an important issue in cardiology. Although conventional coronary angiography is still standard method for assessment of the status of naïve and recipient vessels after CABG surgery, it is an invasive and costly procedure that is not risk-free. Recently, multidetector row computed tomography (MDCT) with retrospective electrocardiographic (ECG) gating has gained rapid acceptance as a diagnostic cardiac imaging modality, allowing assessment of coronary bypass graft patency with high spatial resolution. Initial assessment of bypass grafts was done with single-slice scanners and electron-beam CT. Subsequently, the addition of electrocardiographic ECG gating and the improved capabilities available with 4- or 16-slice MDCT scanners for rapid scanning of the area of interest led to promising results in the imaging of bypass grafts (Marano et al., 2005; Ueyama et al., 1999). Recently, the introduction of 64-slice MDCT permitted improved temporal resolution (94 to 200 msec) and spatial resolution (upto submillimeter) and reduction of both cardiac and respiratory motion, leading to improved assessment of graft stenosis and occlusion (Frazier et al., 2005; Lee et al., 2010). Moreover, 3-dimensional (3D) image processing and advanced volumetric visualization techniques now allow radiologists and cardiologists to evaluate coronary grafts in multiple planes using various projections. With the capability of acquiring 3D data volumes along with its tomographic nature, it shares many of the advantages of intravascular ultrasound and thus has the potential to enhance the practice of percutaneous

*Hyun Suk Yang, Joon Hyung Doh, Hong Jang, Gu Hyun Kang, Yong Hwan Park, Woo Jung Chun, Ju Hyeon Oh, Sung Min Ko and Hweung Kon Hwang

coronary intervention (PCI) in the catheterization laboratory by providing data which was difficult to obtain by invasive coronary angiography (Dikkers et al., 2007; Vembar et al., 2003). Recent studies using 64-slice MDCT have reported sensitivity and specificity values of 95% to 100% and 93% to 100%, respectively, for graft occlusion and high-grade stenosis with > 50% luminal narrowing (Table 1). Since naïve coronary arteries and coronary grafts are small vessels, 2 to 4 mm in diameter, and are characterized by both complex anatomy and continuous movements, high spatial and temporal resolutions are mandatory to visualize these vessels at MDCT. MDCT scanners characterized by submillimeter spatial resolution and a temporal resolution of 94 to 200 ms are now available and are increasingly used for cardiac imaging with promising results.

Authors	MDCT	No. of Patients	No. of Grafts	Sensitivity (%)	Specificity (%)
Achenbach, et al., 1997	Electron-beam	25	56	100	100
Engelmann, et al., 1997	Spiral	49	134	92	97
Marano, et al., 2004	4-MDCT	57	122	89	95
Ropers, et al., 2001	4-MDCT	65	182	92	95
Anders, et al., 2006	16-MDCT	32	94	100	98
Schlosser, et al., 2004	16-MDCT	48	131	96	95
Dikkers, et al., 2007	64-MDCT	34	69	100	99
Jabara, et al., 2007	64-MDCT	50	147	95	100
Nazeri, et al., 2009	64-MDCT	89	287	98	97
Ropers, et al., 2006	64-MDCT	50	138	100	94
Tochii, et al., 2010	64-MDCT	19	90	100	93

High-grade stenosis is defined as 50-99% stenosis

Table 1. Results of studies of the use of MDCT to evaluate occlusion and high-grade stenosis of grafts

2. Imaging acquisition

2.1 Image protocol

There are a variety of protocols for image acquisition in the evaluation of patients after CABG surgery. In many respects, the protocol is similar to that for coronary CT angiography (CTA). One important difference is that the scan should be extended superiorly to include the origins of the internal mammary arteries. Scanning is performed with the patient in the supine position, during breath-hold. After placement of the leads for ECG recording on the chest wall and a check of the heart rate, a noncontrast CT scan image is acquired through the entire thorax in order to define the volume of the subsequent CT angiography and to detect associated or unsuspected findings. Hence, MDCT angiography is performed during ECG recording, from the subclavian arteries to the cardiac base; in patients with venous grafts, a smaller scanning volume starting from the lower third of the ascending aorta is usually sufficient. On the contrary, when a right gastroepiploic artery (RGEA) has been used, the scanning volume should include the upper abdomen. Cardiac CTA technique requires rapid injection of nonionic, iodinated, low-osmolar intravenous

contrast. A bolus of 100 to 120 mL nonionic contrast material (high iodine concentration is recommended) is administered intravenously using an automatic injector at a flow rate of 3 to 4 mL/s. A region of interest was placed in the descending aorta by using a preset threshold of 150 HU; a 10-second delay followed before scanning was begun to ensure filling of the distal vessels with contrast material. Since the left internal mammary artery (LIMA) is the most frequently used graft to the anterior cardiac wall, a right arm venous access is preferable in order to avoid streak artifacts from the left subclavian vein that may hamper a complete evaluation of LIMA course and takeoff. Axial images are reconstructed in the mid-to-late diastolic phase, using a fraction (percentage; relative delay) of the R-R interval of the cardiac cycle. Images are acquired with a heart rate < 70 beats per minute, if possible, and with breath-holding during mid-inspiration to prevent substantial inflow of unopacified blood into the right atrium, which may result in heterogeneity of contrast. Low heart rates (< 65 beats/min for 16-slice MDCT or < 70 beats/min for 64-slice MDCT) are recommended to obtain high-quality CT scans, and in the absence of contraindications (heart failure, systolic BP < 100 mm Hg, atrioventricular blockade greater than grade I, and referred adverse reaction), beta-blockers can be administered before CT acquisition (Frazier et al., 2005; Marano et al., 2005). Oral or intravenous beta-adrenergic blocking medications, specifically metoprolol (Lopressor; Novartis Pharmaceuticals Corp., East Hanover, NJ), are administered prior to scanning to prevent heart rate variability and tachycardia. Retrospective ECG-gated CTA is essential for optimal image acquisition and reconstruction of evenly spaced phases of the cardiac cycle. The images are acquired in a limited field of view with axial images centered on the heart. Using 60% to 80% of the R-R interval, with 0.6-0.75 mm thick images reconstructed in 0.4-0.5 mm increments, axial source images, three-dimensional (3D) volume-rendered images, and multiplanar reformatted (MPR) images are generated. Both 3D volume-rendering and MPR images are used to assess the bypass grafts, proximal and/or distal graft anastomoses, and the cardiac anatomy. In particular, curved multiplanar images with centerlines through the bypass grafts and native coronary arteries are obtained. To correctly assess graft patency and/or the presence of significant stenosis and occlusion, a thorough knowledge of CABG anatomy and its configuration on CTA is important for radiologists and cardiologists. There are 2 types of bypass grafts, arterial and venous. Venous grafts are generally larger in caliber than arterial grafts, and for this reason, jointly to the absence of surgical clips along their course, venous grafts are usually better assessable by noninvasive imaging techniques. In order of frequency of use, graft arteries include the internal mammary arteries (IMAs), radial arteries (RAs), right gastroepiploic artery (RGEA), and inferior epigastric artery (IEA). Although arterial grafts have better long-term outcomes, venous grafts, specifically saphenous vein grafts (SVGs), are more readily available. CTA following CABG surgery is done by first assessing the morphology and size of the ascending aorta and the origin of the in situ vessel such as the IMA. Then, graft patency is assessed for homogeneous, contrast-enhanced graft lumen and for regular shape and border of the graft wall. The graft is usually divided into 3 different segments: the origin or proximal anastomosis of the graft, the body of the graft, and the single (or sequential) distal anastomosis. During the CTA evaluation of bypass grafts, the proximal anastomosis is usually better visualized than the distal anastomosis. In cases in which the distal anastomosis is not well evaluated, the bypass graft is usually considered patent as long as contrast is evident within the graft lumen.

2.2 Image noise

The advantages of MDCT are the relatively rapid imaging time and high spatial resolution attributable to the multi-row detector system. Numerous studies dealing with MDCT coronary bypass angiography have reported cardiac and respiratory motion artifacts as the most significant limitations in the reliable assessment of graft patency and stenosis of recipient vessels. It is well known that heart rate greatly influences image quality and stenosis detection. The introduction of 64-slice MDCT scanners, with faster gantry rotation times and shorter breath-hold times, improved diagnostic image quality by reducing cardiac and respiratory motion artifacts. However, optimum performance was observed primarily in patients with heart rates below 70 beats per minute. Even with improved spatial and temporal resolution with 64-slice technology, routine administration of β-blockers is still required. If graft segment image quality is suboptimal due to motion artifacts, a potential remedy is to obtain additional image reconstructions in smaller increments throughout the cardiac cycle. The other limitations of MDCT are the presence of calcification and metal clip artifacts, which make assessment of graft patency difficult, and accurate evaluation of the degree of stenosis impossible. Nevertheless, the thinner slices of 64-slice MDCT give increased temporal resolution, and 3-dimentional reconstructions show consistent detail in every plane. Moreover, bypass grafts are characterized by minor calcification compared to naive vessels, allowing more accurate analysis in most cases. Coronary calcifications and metal clip artifacts still remain a challenging issue with 64-slice cardiac CT despite improvements with the use of sharper image filters, e.g. the B46 Kernel (Siemens Medical Solutions) (Seifarth et al., 2005). The another important limitation is the high radiation dose required for 64-slice MDCT, although electrocardiogram-dependent dose modulation can reduce this by 30%–50%. The minimization of radiation exposure as well as optimization of the diagnostic accuracy in calcified vessels remain the chief goals for future MDCT advances.

3. Type of arterial or vein graft

3.1 Saphenous Vein Graft (SVG)

The SVG was first successfully used in a CABG operation by Sabiston in 1962. Both the benefits and limitations of SVG have been well documented in the literature (Bourassa et al., 1985; Campeau et al., 1983). Saphenous veins are fairly simple to access and harvest from the lower extremities, and they are more versatile and widely available than arterial grafts. In addition, during the intra- and perioperative period, saphenous veins are resistant to spasm versus their arterial counterparts. However, the use of SVG is limited by distortion from varicose and sclerotic disease as well as a higher occurrence of intimal hyperplasia and atherosclerotic changes after exposure to systemic blood pressure, resulting in lower patency rates. Graft occlusion can also occur due to vascular damage during harvesting of the saphenous vein. In a large study, the SVG patency was 88% perioperatively, 81% at 1 year, 75% at 5 years, and 50% at greater than or equal to 15 years (Fitzgibbon et al., 1996). The graft attrition rate between 1 and 6 years after CABG surgery is 1% to 2% per year, and between 6 and 10 years is 4% per year. The great saphenous vein is the vein routinely used for CABG surgery. The proximal anastomosis of the venous graft with the ascending aorta is usually performed cranial to the origin of coronary arteries and as distal as the proximal portion of the aortic arch. The SVG can be sutured directly to the anterior portion of the ascending aorta or attached with an anastomotic device, allowing faster, sutureless

attachment. The device, called the Symmetry Bypass System aortic connector (St Jude Medical, St Paul, Minn), alters the common appearance of the bypass graft by requiring the aortic connector to be anastomosed perpendicularly to the aorta (Mack et al., 2003; Poston et al., 2004). Recent reports have documented the development of significant stenosis and occlusion in 13.7%-15.5% of vein grafts attached with the aortic connector (Carrel et al., 2003; Wiklund et al., 2002). In order to support the course of the aortovenous anastomosis, the left-sided SVG is connected to the left side of the aorta, stabilizing the graft on top of the main pulmonary artery. A right-sided SVG is attached either to the lower aspect or right side of the ascending aorta, allowing the graft to traverse the right arterio-ventricular groove. SVGs tend to appear as large contrast-filled vessels (Fig.1).

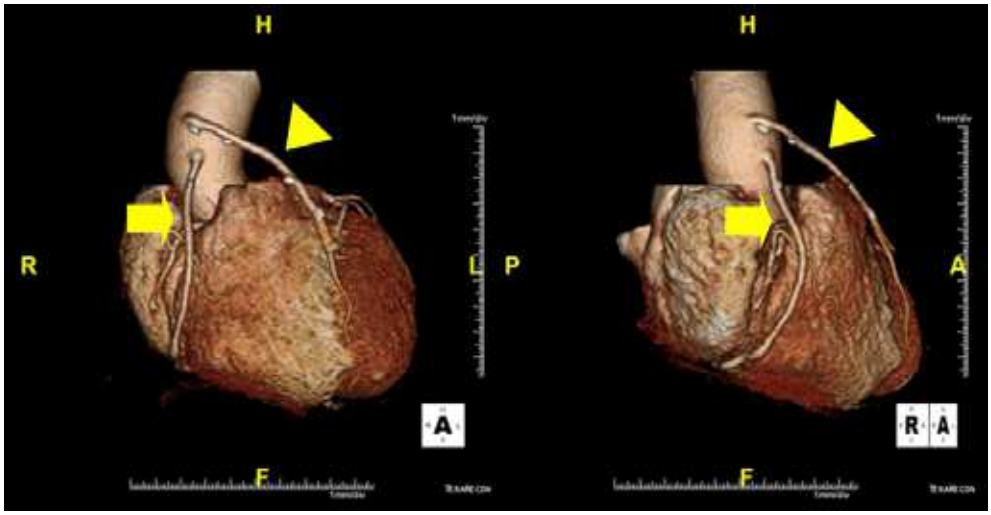

Fig. 1. Saphenous vein grafts. Three-dimensional volume-rendered images show the typical appearance of right (arrow) and left (arrowhead) saphenous vein grafts (SVGs) sutured to the anterior aorta. The left SVG is attached to the mid-portion of left anterior descending (LAD) artery and the right SVG is attached to the distal-portion of right coronary artery (RCA).

An SVG to the right side is attached to the distal right coronary artery (RCA), posterior descending artery (PDA), or distal LAD artery. The distal anastomosis may lie on the phrenic wall of the heart. An SVG to the left side is attached distally to the LAD artery, diagonal artery, left circumflex (LCx) artery, or the obtuse marginal (OM) arteries, by traversing anteriorly and superiorly to the right ventricle outflow tract (RVOT) or main pulmonary artery (Fig. 2, 3, 4).

SVG may present a horizontal or slightly oblique course on axial images, especially when the distal anastomosis is placed on the LCx or a diagonal branch to supply the left cardiac wall. In these cases, the graft can be recognized in the fatty tissue of mediastinum, posterior to the sternum and anterior to the RVOT. On occasion, the distal SVG is anastomosed sequentially to greater than or equal to 2 coronary vessels or in the same vessel, using side-to-side and end-to-side anastomoses. The naive vessel distal to the anastamotic site should be assessed and is recognized by its position and smaller caliber compared with the SVG

(Fig. 3, 4). Typically, venous grafts are larger than arterial grafts and are not accompanied by surgical clips along their course. Sometimes a circumferential clip can be identified at the site of proximal anastomosis with the ascending aorta (Fig.1).

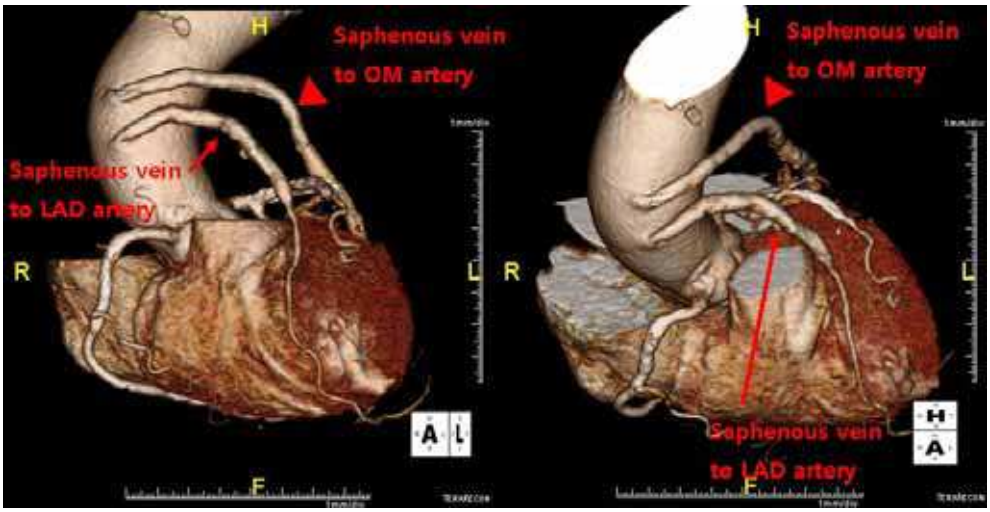

Fig. 2. Saphenous vein grafts. Three-dimensional volume-rendered images show the typical appearance of right (arrow) and left (arrowhead) saphenous vein grafts (SVGs) sutured to the anterior aorta. The right SVG is attached to the mid-portion of left anterior descending (LAD) artery and the left SVG is attached to the obtuse marginal (OM) artery

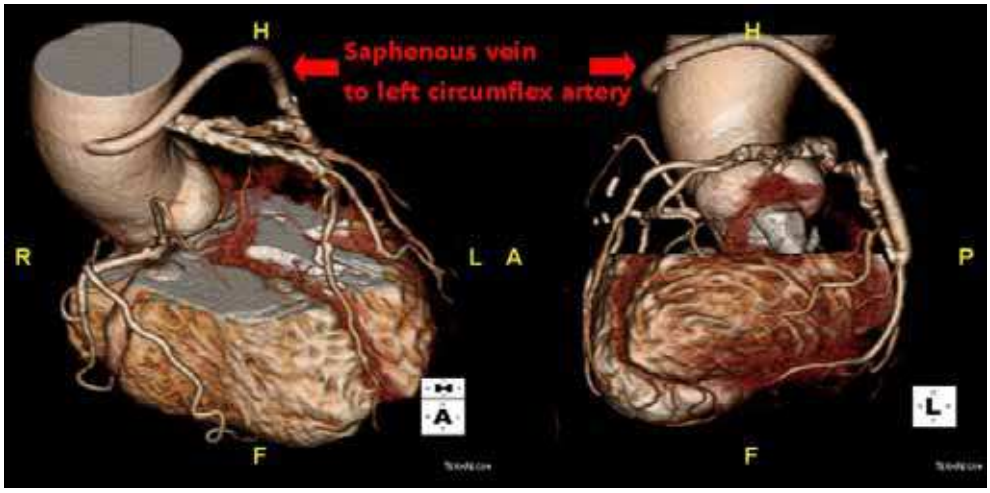

Fig. 3. Saphenous vein graft. Three-dimensional volume-rendered images show the left saphenous vein graft (SVG) with its anastomosis with the left circumflex (LCx) artery.

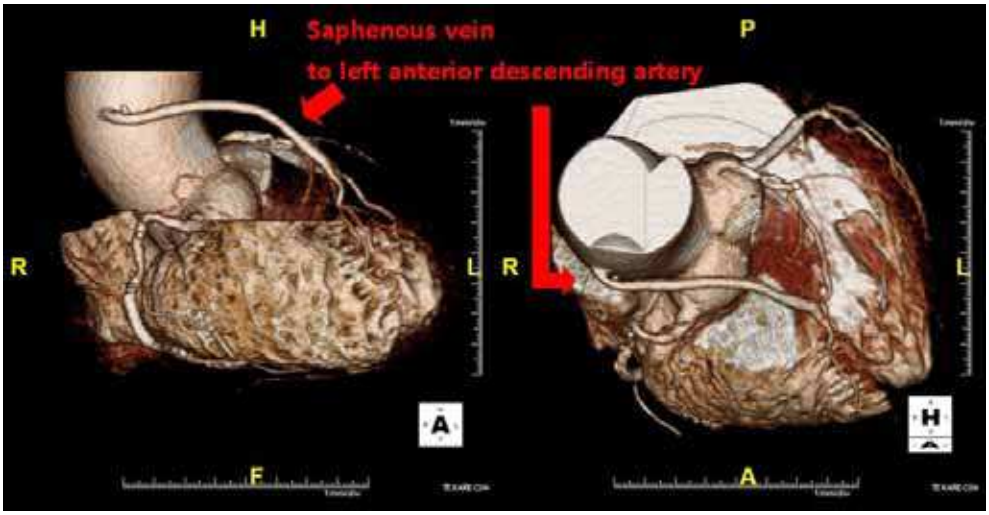

Fig. 4. Saphenous vein graft. Three-dimensional volume-rendered images show the left saphenous vein graft (SVG), which is attached to the mid-portion of left anterior descending (LAD) artery.

3.2 Internal Mammary Artery (IMA)

The internal mammary artery (IMA) is characterized by unique resistance to atherosclerosis and extremely high long-term patency rates compared with the saphenous vein. The IMA has a nonfenestrated internal elastic lamina without vaso vasorum inside the vessel wall, which tends to protect against cellular migration and intimal hyperplasia. Moreover, the medial layer of IMA is thin and poor of muscle cells with poor vasoreactivity. In addition, the endothelium produces vasodilator (nitric oxide) and platelet inhibitor (prostacyclin). Glycosaminoglycan and lipid compositions of IMA result in being less atherogenetic in comparison with venous grafts. Therefore, use of the IMA decreases all postoperative cardiac events and mortality, and is associated with a long-term patency rate well >90% at 10 years (Loop et al., 1986; Motwani & Topol, 1998).

3.2.1 Left IMA

The Left IMA (LIMA) is the vessel of choice for the surgical revascularization of the left anterior descending (LAD) artery for its biological and anatomical characteristiscs, being the conduit more proximal to the LAD artery and the easiest to harvest both in median sternotomy and mini-thoracotomy. Due to anatomical proximity to the LAD artery and favorable patency rates, the left IMA (LIMA) is most commonly used as an in situ graft to revascularize the LAD or diagonal artery, supplying the anterior or anterolateral cardiac wall. The LIMA extends from its origin at the subclavian artery and courses through the anterior mediastinum along the right ventricle outflow tract (RVOT) after being separated surgically from its original position in the left parasternal Region (Fig. 5).

Infrequently, sequential distal anastomoses, with side-to-side and end-to-side anastomoses to the diagonal and LAD arteries, respectively, or involving separate sections of the LAD artery, are performed. On axial images, the LIMA is no longer visible in its usual site, on the

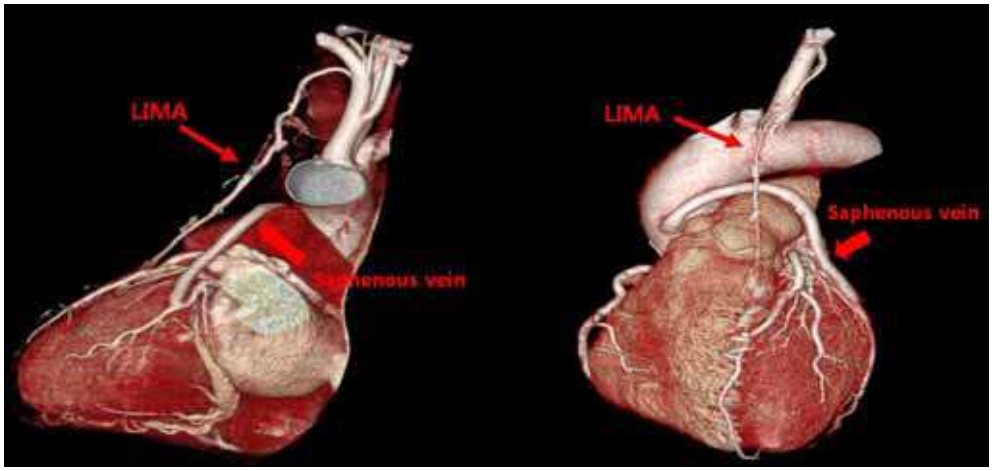

Fig. 5. Left internal mammary artery (IMA) graft. Three-dimensional volume-rendered images show the left IMA graft from its origin at the left subclavian artery to its anastomosis with the left anterior descending (LAD) artery. There is also a left saphenous vein graft (SVG), which is attached to the obtuse marginal (OM) artery. Note the smaller diameter of the arterial graft compared with that of the venous graft.

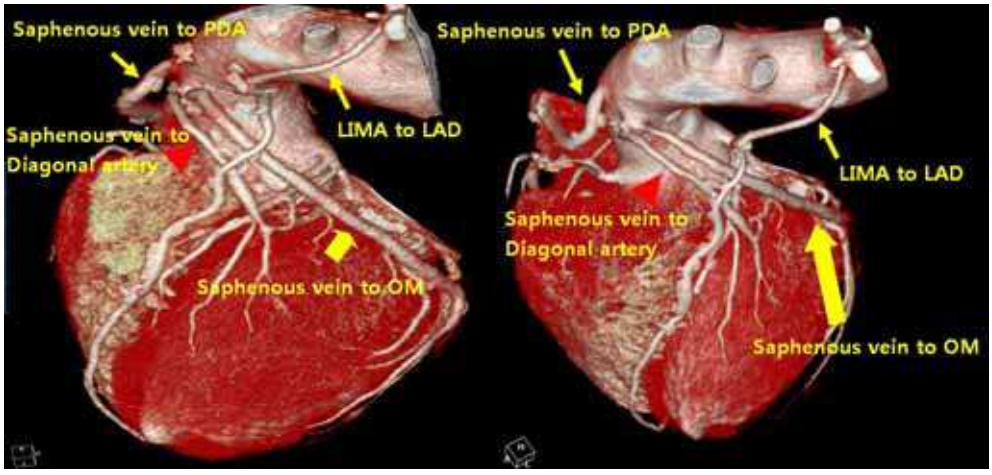

Fig. 6. Left internal mammary artery (IMA) graft. Three-dimensional volume-rendered images show the left IMA graft from its origin at the left subclavian artery to its anastomosis with the left anterior descending (LAD) artery. There is also a right saphenous vein graft (SVG) sutured to the anterior aorta with its anastomosis with the posterior descending artery (PDA). The left saphenous vein grafts (SVG) are attached to diagonal artery and the obtuse marginal (OM) artery.

left side of the sternum, but courses as a small vessel in the anterior mediastinum along the right ventricle outflow tract (RVOT). Although in most cases LIMA grafts show a single distal anastomosis to the left anterior descending artery (LAD) or a diagonal branch, multiple sequential anastomoses to both the LAD and diagonal branches are sometimes performed. Surgical clips are routinely used to occlude collaterals and to avoid arterial bleeding and can be seen either adjacent to the graft or at the original site of the LIMA. As with other grafts, on CTA, the distal anastamosis is typically most difficult to visualize. Surgical clips are used routinely to occlude branch vessels of the IMA, and metallic artifact may limit assessment in some instances (Fig. 6).

3.2.2 Right IMA

The right IMA (RIMA) is used less frequently than the LIMA. The RIMA may be used in a variety of ways. As an in situ graft, The RIMA remains attached to the right subclavian artery proximally and anastomoses with the target coronary artery distally. However, it is more commonly used as "free" graft from the ascending aorta to the RCA or from the LIMA to the left circumflex artery (LCx) or obtuse marginal (OM) branches. In cases in which both in situ IMAs are necessary for revascularization of the left heart, either the RIMA is connected to the LCx artery or OM branches by extension through the transverse sinus of the pericardium and the LIMA is attached to the LAD artery or the RIMA is attached to the LAD artery and the LIMA is anastomosed to the LCx artery or other side branches (OM or diagnonal branches). Otherwise, the RIMA can be removed from the right subclavian artery and used as a composite or free graft. As a segment of a composite graft to perform an arterial "T" or "Y" graft, the RIMA is anastomosed proximally to LIMA, allowing total arterial revascularization instead of using a venous graft with LIMA. As a free graft, a RIMA is anastomosed to the anterior ascending aorta and used in the same way as an SVG. The CTA appearance of the RIMA is similar to that of the LIMA. As already described for LIMA grafts, surgical clips are used to occlude collaterals. Studies have shown that total arterial myocardial revascularzation has the advantages of decreased recurrent angina and superior patency rates at 1 year when compared with those of conventional coronary artery bypass surgery in which a LIMA graft is coupled with an SVG (Muneretto et al., 2003).

3.3 Radial Artery (RA)

The first use of the radial artery (RA) as arterial conduit for coronary revascularization has been de-scribed by Carpentier et al in 1971 (Carpentier et al., 1973). As a muscular artery from the forearm, the RA has a prominent medial layer and elevated vasoreactivity, which results in a lower patency rate than that of IMA grafts (Possati et al., 2003). The RA is usually harvested from the nondominant arm and is used as a third arterial graft, either as a free or composite graft or to avoid using a venous graft in case of unavailability of IMA grafts. The RA is often grafted to supply the left cardiac wall (LCx, OM). On CTA, the caliber of the RA is similar to the IMA, but it typically is visualized coursing from the ascending aorta to the naïve coronary artery (Fig. 7). In the early postoperative period, the RA may be reduced in caliber and may be difficult to identify because of vasospasm. In addition, because the RA is a muscular artery, the number of surgical clips used to close collaterals along the graft is usually higher than with IMA. This may represent a limit for noninvasive assessment of RA grafts with MDCT because of artifacts from surgical clips limiting a full CTA evaluation of an RA graft.

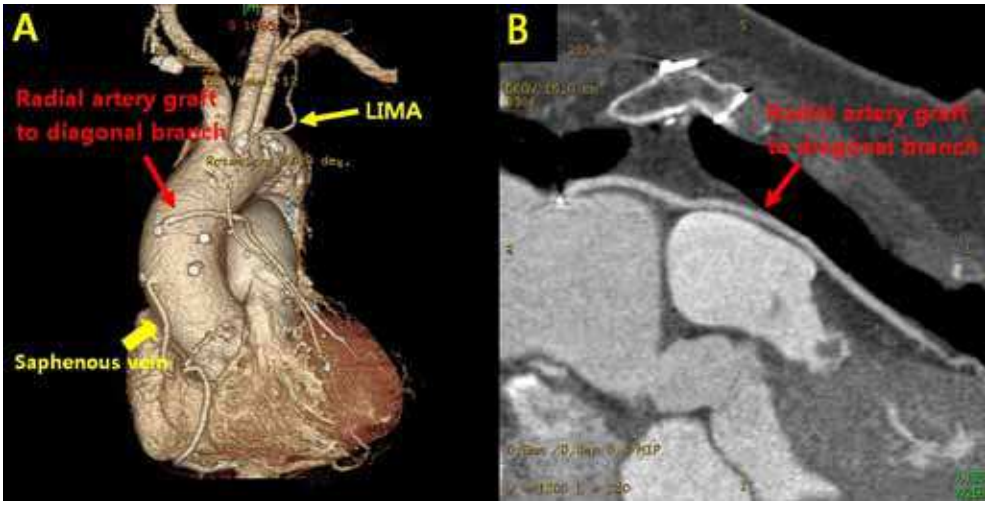

Fig. 7. Radial artery (RA) graft. (A) Three-dimensional volume-rendered image shows radial artery graft sutured to the anterior aorta with its anastomosis with diagonal artery. There are also left internal mammary artery (LIMA) graft from its origin at the left subclavian artery to its anastomosis with the left anterior descending (LAD) artery and right saphenous vein graft (SVG), which is attached to the distal right coronary artery (RCA). Note the diameter of the RA is similar to the IMA, but it typically is visualized coursing from the ascending aorta to the diagonal artery. (B) Curved multiplanar reformation image shows patent RA graft within the anterior mediastinum. The full extent of the graft is seen from the ascending aorta to diagonal artery.

3.4 Right Gastroepiploic Artery (RGEA) and Inferior Epigastric Artery (IEA)

The use of right gastroepiploic and inferior epigastric arteries in CABG procedures has been limited because of the need to extend the median sternotomy to expose the abdominal cavity (Buche et al., 1992; Manapat et al., 1994; Pym et al., 1987). Although the use of these arteries increases surgical time and technical difficulty of the surgery, these arteries can be used as a free graft to perform total arterial revascularization. The use of the RGEA was first described by Pym et al in June 1984 (Pym et al., 1987). Although it has been originally used in reoperation, in the absence of other suitable conduits, RGEA is now used as secondary, tertiary, or quaternary arterial conduit to provide all-arterial revascularization. The biological characteristics of RGEA are similar to IMA, but unclear benefits for third or fourth arterial grafts, the increment of surgery time, and the involvement of an additional body cavity are the main drawbacks limiting the widespread use of this conduit. Occasionally, the RGEA is used to supply the inferior cardiac wall and is anastomosed as an in situ graft to the posterior descending artery (PDA). In these cases, the mobilized artery is seen coursing anterior to the liver and through the diaphragm to reach the site of anastomosis. Small clips can be identified at the original site of the RGEA, near the small curvature of stomach. These instances require that the surgical history be conveyed to the radiologist so the CTA protocol can be modified to include the upper abdomen, because the gastroepiploic artery is freed to course anteriorly to the liver and through the diaphragm to reach the target vessel. The inferior epigastric artery (IEA) is an arterial branch of the abdominal wall, arising from

the external iliac artery and coursing inside the abdominal rectus muscle. Similar to the radial artery (RA), the IEA has a predominant muscular structure, while the limited length of the vessel with an adequate caliber is a constraint to using this vessel only as a lateral branch of a multiple arterial graft.

4. Planning percutaneous intervention (PCI) or repeat surgery of bypass graft

As medical and surgical treatments for coronary artery disease have improved, patients are living longer. Consequently, PCI or second CABG operations have become more common. Sometimes, because the proximal anastomosis of the bypass grafts with the aorta is occluded or severe stenotic, visualization of bypass grafts is difficult or impossible with invasive coronary angiography, and if it is possible, the radiation dose must be increased for visualization of the grafts and naive vessels. MDCT is emerging as a useful tool of mapping the course of bypass grafts before PCI (Dikkers et al., 2007; Hecht & Roubin, 2007; Song et al., 2010). Three-dimentional volume-rendered images with computer software delineate relationships between the aorta, naïve arteries, and bypass grafts. Figure 8 (Song et al., 2010) is an example of successful PCI for occluded coronary artery bypass grafts with the aid of MDCT. A 68-year-old man was admitted to our hospital with severe exertional chest pain of 2 months duration. He had been diagnosed with unstable angina 2 years earlier. At that time, coronary angiography had revealed severe 3-vessel disease with diffuse 50% stenosis from the distal portion of the left main coronary artery to the left anterior descending coronary artery (LAD), diffuse 90% stenosis of the left circumflex artery, and total occlusion of the obtuse marginal (OM) branches and proximal right coronary artery. Subsequently, CABG had been performed using left internal mammary artery to the LAD, saphenous vein for aorta-diagonal-OM1-OM2 grafts, and free right internal mammary artery to the posterior descending coronary artery. In invasive coronary angiography, the left internal mammary artery-to-LAD graft was patent, but no aortic ostium could be seen despite repeated attempts with various catheters and aortography. Because conventional angiography failed to visualize the grafts, we examined the feasibility of a PCI using 64-slice MDCT. The aortic graft anastomosis was totally occluded, but there was no vessel wall calcification. All grafted vessels could be identified. Based on these findings, a successful second-stage PCI was performed. Injury to a preexisting left IMA graft at sternal reentry is a well-recognized risk in second CABG surgery (Fullerton et al., 1994; Gillinov et al., 1999). MDCT is emerging as a useful means of mapping the course of a left IMA graft before repeat surgery (Gilkeson et al., 2003; Ohtsuka et al., 2000). Three-dimensional volume-rendered images delineate relationships between the sternum, ribs, and bypass grafts, thereby minimizing the risk of injury to the graft vessel during surgical reentry. Understanding the sternal proximity of preexisting bypass grafts, as well as normal structures including the aorta, pulmonary artery, and naïve coronary arteries, allows the surgeon to plan an appropriate surgical approach.

5. Complication

5.1 Graft failure

Bypass graft failures are classified either as early or late following CABG surgery. During the early phase, usually within 1 month after CABG surgery, the most common cause of graft failure is thrombosis from platelet dysfunction at the site of focal endothelial damage

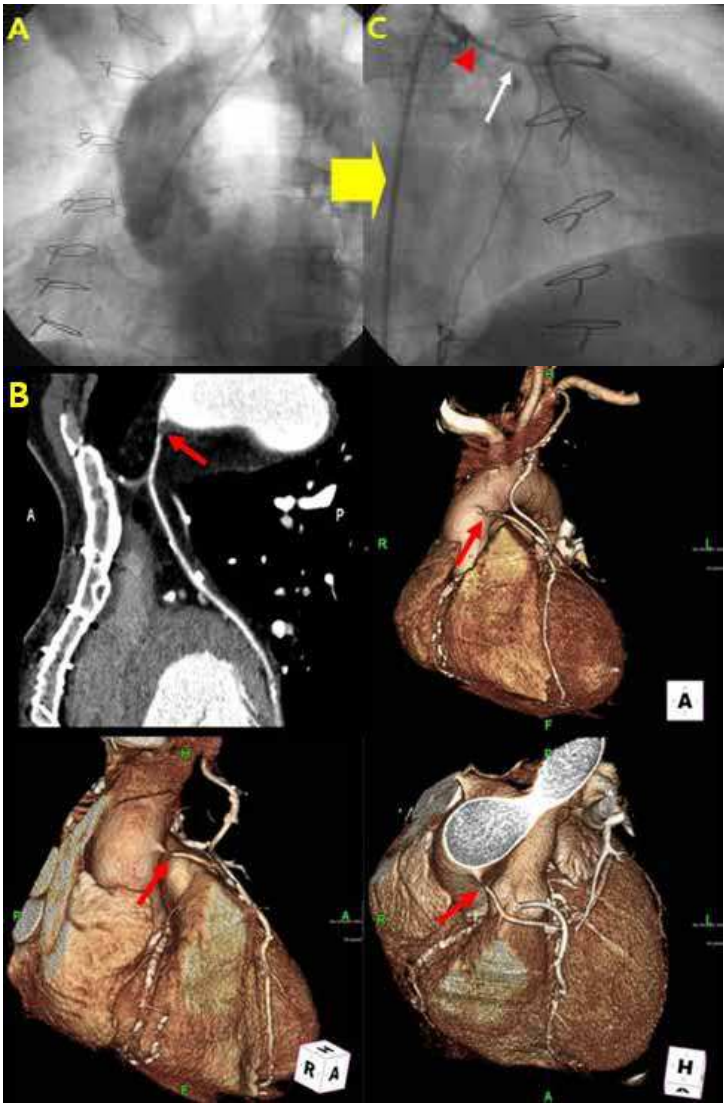

Fig. 8. Coronary artery graft dilatation aided by multidector computed tomography. (A) In invasive coronary angiography, aortic ostium of saphenous vein graft (SVG) could not be seen despite repeated attempts with various catheters and aortography. (B) Curved multiplanar reformation image and three-dimensional volume-rendered image showed the aortic graft anastomosis of saphenous vein graft (SVG) was totally occluded. There was also a patent left internal mammary artery (LIMA) graft from its origin at the left subclavian artery to its anastomosis with the left anterior descending (LAD) artery. (C) Based on these 64-MDCT findings, a second-stage percutaneous coronary intervention (PCI) was performed successfully. Note that 64-MDCT is a useful tool for visualizing bypass graft in a selected group of patients with failed angiography for graft assessment.

during surgical harvesting and anastomosis. Graft closure from thrombosis at 1 month is a recognized complication in 10-15% of cases (Fitzgibbon et al., 1996). Perioperative venous graft failure after off-pump CABG procedures is chiefly determined by the two factors of graft endothelial damage and patient hypercoagulability. Early bypass graft failure can also be due to a malpositioned graft (Ricci et al., 2000). If the graft is too long, it may twist or kink. Technical factors associated with use of an aortic connector may predispose venous

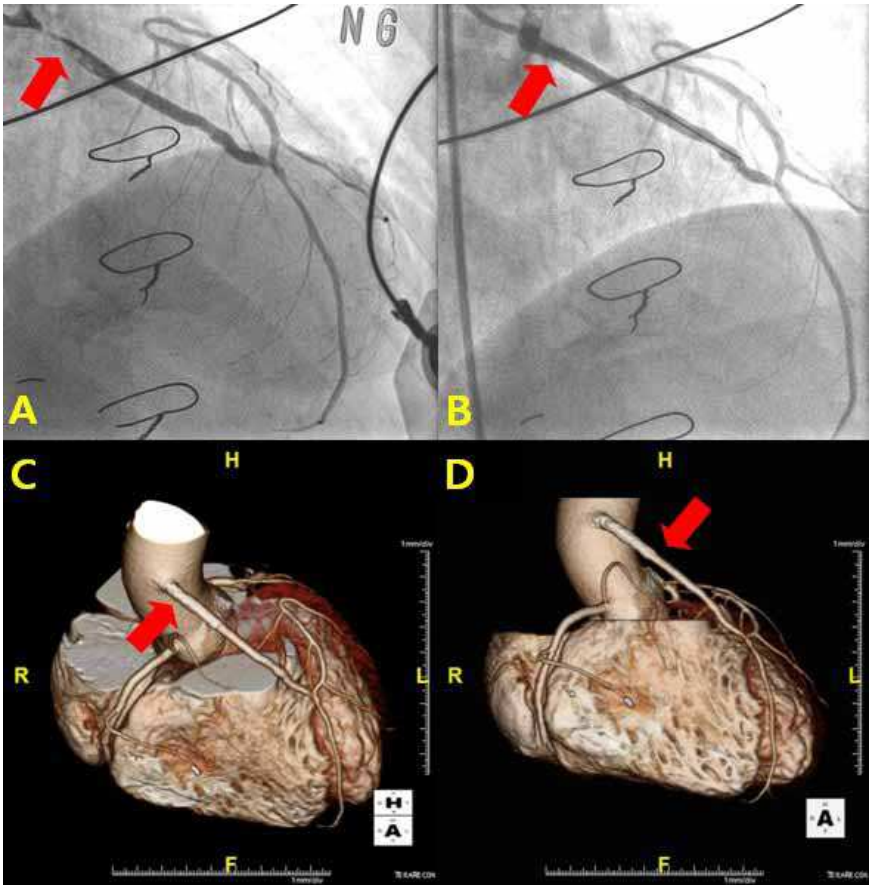

Fig. 9. Acute occlusion of saphenous vein graft (SVG). (A) Invasive coronary angiography showed the proximal-portion of saphenous vein graft (SVG) was severely occluded with thrombi. (B) After successful percutaneous coronary intervention (PCI), invasive coronary angiography showed the proximal-portion of saphenous vein graft (SVG) with stenting was patent. (C, D) At 6-month follow-up, three-dimensional volume-rendered image showed the proximal-portion of saphenous vein graft (SVG) with stenting was still patent. Note that the findings of invasive coronary angiography is similar to those of three-dimensional volume-rendered images of 64-MDCT. The figures also demonstrate that 64-MDCT has a useful role to follow-up of patients who have undergone percutaneous intervention for bypass graft stenosis and occlusion.

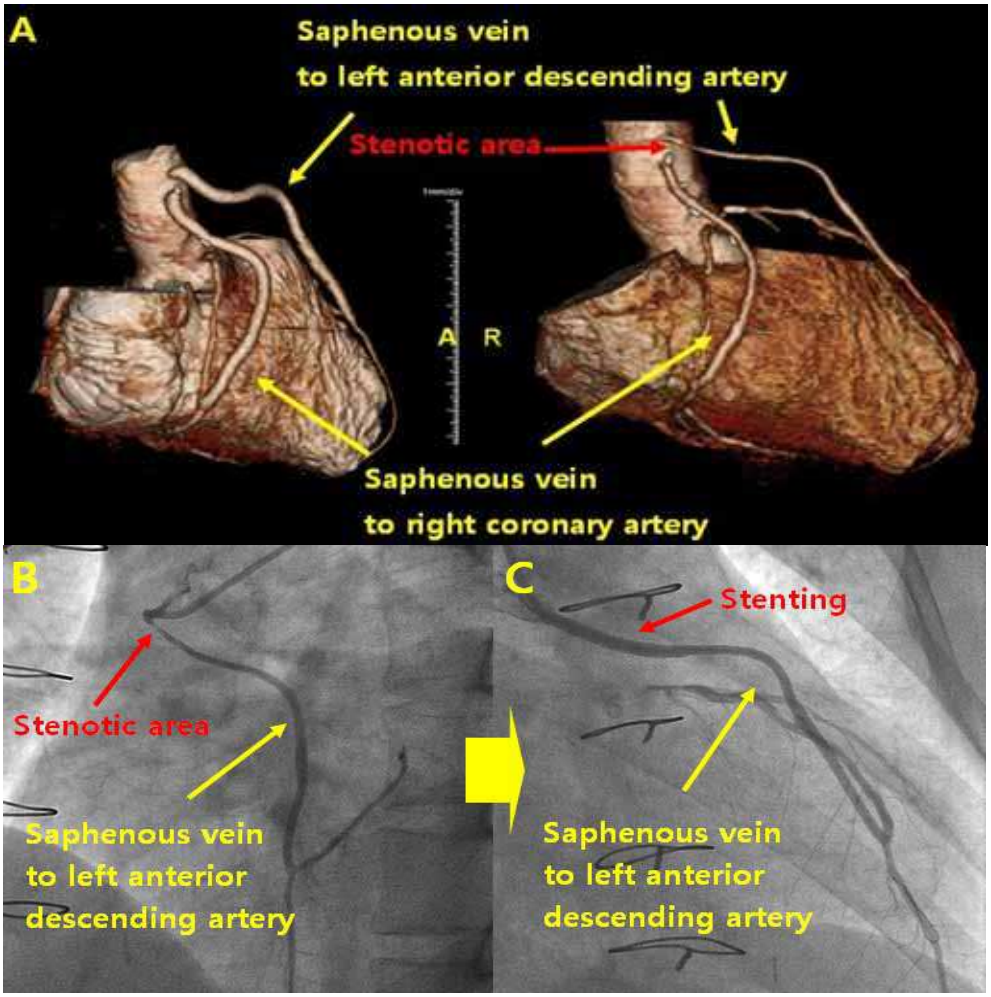

Fig. 10. Chronic occlusion of left saphenous vein graft (SVG). (A, left panel) Immediate after CABG surgery, three-dimensional volume-rendered image showed that left saphenous vein graft (SVG) was patent with its anastomsis to the mid-portion of left anterior descending (LAD) artery. There was a patent right saphenous vein graft (SVG), which was attached to the distal-portion of right coronary artery (RCA). (A, right panel) At 8 months after CABG surgery, three-dimensional volume-rendered image showed severe stenosis at proximal-portion of left saphenous vein graft (SVG), which was attached to the mid-portion of left anterior descending (LAD) artery. Right saphenous vein graft (SVG) was still patent despite the graft had diffuse mild narrowing from proximal anastomosis site to distal anastomosis site. (B) Invasive coronary angiography showed the proximal-portion of left saphenous vein graft (SVG) was severely occluded. (C) Percutaneous coronary intervention was performed successfully. Note that the findings of invasive coronary angiography is similar to those of three-dimensional volume-rendered images of 64-MDCT.

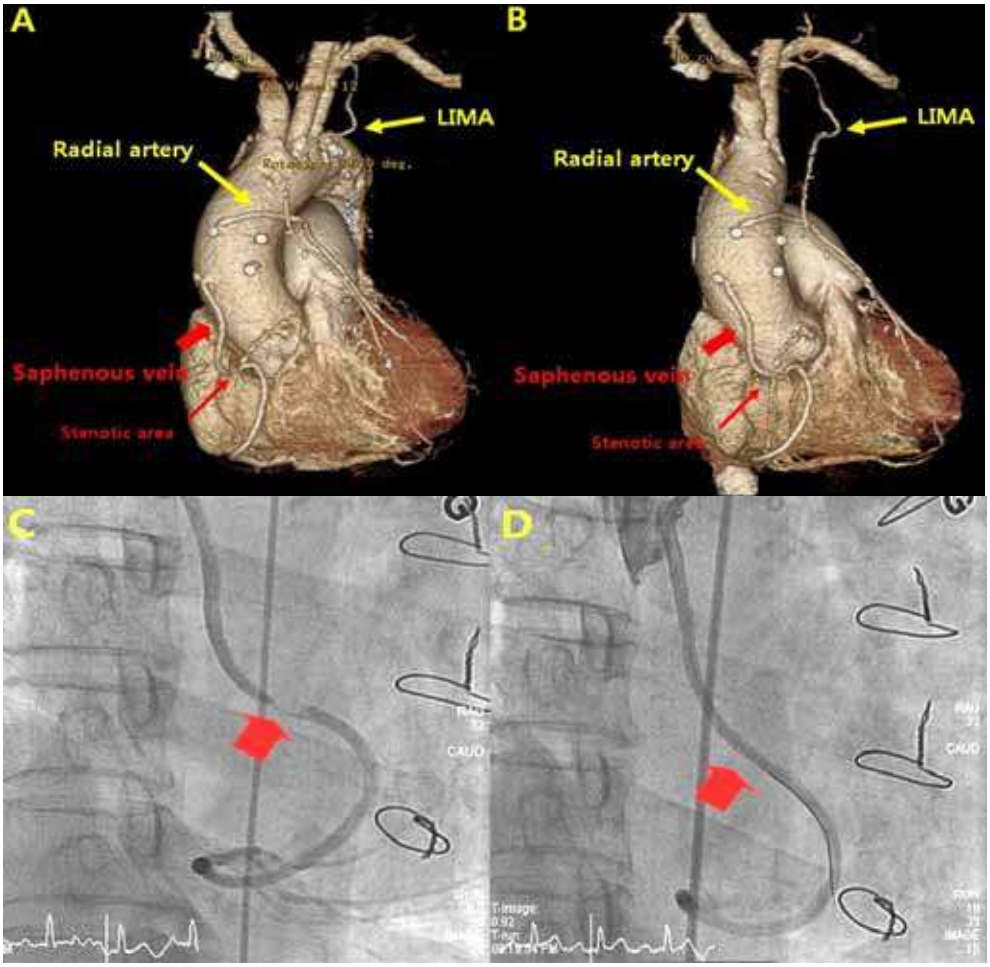

Fig. 11. Chronic occlusion of right saphenous vein graft (SVG). (A, B) Three-dimensional volume-rendered image showed severe stenosis at mid-portion of right saphenous vein (SVG) graft, which is attached to the distal right coronary artery artery (RCA). Radial artery (RA) and left internal mammary artery (LIMA) grafts were patent. (C) Invasive coronary angiography showed the mid-portion of right saphenous vein (SVG) graft was severely occluded. (D) Percutaneous coronary intervention was performed successfully. Note that the findings of invasive coronary angiography is similar to those of three-dimensional volume-rendered images of 64-MDCT.

grafts to kinking (Traverse et al., 2003). Late-phase venous graft failure is due primarily to progressive changes related to systemic blood pressure exposure. One month after surgery, the venous graft starts to undergo neointimal hyperplasia. Although this process does not produce significant stenosis, it is the foundation for later development of graft atheroma. Beyond 1 year, atherosclerosis is the dominant process, resulting in graft stenosis and occlusion. On the other hand, arterial grafts, specifically IMA graft, are resistant to atheroma

development. Late IMA graft failure is more commonly due to progression of atherosclerotic disease in the native coronary artery distal to the graft anastomosis. CTA can delineate multiple findings associated with graft stenosis and occlusion. Calcified and noncalcified atherosclerotic plaque is readily identified, and the calculation of the extent of graft narrowing is straightforward. Occlusion can be determined by non-visualization of a vessel which is known to have been used for surgical grafting. In many instances, the most proximal part of an occluded aortocoronary graft fills with contrast, creating a small out-pouching from the ascending aorta, allowing a diagnosis. Acute or chronic graft occlusion can sometimes be differentiated by the diameter of the bypass graft. In chronic occlusion, the diameter is usually reduced from scarring, as compared with acute occlusion in which the diameter is usually enlarged (Fig. 9, 10, 11).

5.2 Graft vasospasm

Radial artery (RA) grafts are susceptible to vasospasm because the RA is a muscular artery with elevated vasoreactivity. The appearance is similar to fixed graft stenosis, although the luminal narrowing is more extensive in length. Nevertheless, the administration of intraoperative alpha-adrenergic antagonist solution or posteroperative calcium channel blockers can overcome many cases of graft vasospasm postoperatively (Locker et al., 2002; Myers & Fremes, 2003).

5.3 Graft aneurysm

There are 2 types of bypass graft aneurysms: true aneurysms and pseudoaneurysms (Dubois & Vandervoort, 2001; Mohara et al., 1998). True aneuryms are usually found 5 to 7 years after CABG surgery and are related to atherosclerotic disease. On the other hand, pseudoaneuryms more commonly occur within 6 months after surgery, although they may also arise several years later. Pseudoaneurysms arise at either proximal or distal anastomotic sites. Pseudoaneurysm cases that are found earlier may be related to infection or tension at the anastomotic site, resulting in suture rupture. In late-onset pseudoaneurysms, similar to true aneurysms, atherosclerotic changes likely played a role. Currently, there is no clear guideline for surgery. Nevertheless, size >2 cm has been a cause for concern (Memon et al., 2003). Graft aneurysms may lead to various complications, including compression and mass effect on adjacent structures, thrombosis and embolization of the bypass graft leading to an acute coronary event, formation of fistula to the right atrium and ventricle, sudden rupture leading to hemothorax, hemopericardium, or death.

5.4 Pericardial and pleural effusions

Approximately 22%-85% of patients have postoperative pericardial effusions after CABG surgery (Meurin et al., 2004; Pepi et al., 1994). Although pericardial effusions are common, only 0.8%-6% of patients progress to cardiac temponade (Katara et al., 2003). Risk factors include postoperative coagulation abnormality or use of anticoagulation agents that are often related to the use of cardiopulmonary bypass. Nearly all significant pericardial effusions are diagnosed within 5 days postoperatively, peak in 10 days, and resolve within a month (Kuvin et al., 2002). Postoperative pleural effusions are even more numerous after surgery, a prevalence of 89% within 7 days after surgery (Hurlbut et al., 1990; Vargas et al., 1994). These pleural effusions are usually unilateral, small, left-sided, and without clinical

significance. Only 1%-4% of CABG surgery patients proceed to develop clinically significant effusions that require thoracentesis (Peng et al., 1992).

5.5 Sternal infection

The sternal infection is an important complication of the CABG surgery, with a prevalence of 1% to 20% (Roy, 1998). Three different compartments may be affected: the presternal (cellulitis, sinus tracts, and abscess), sternal (osteomyelitis, and dehiscence), or retrosternal (mediastinitis, hematoma, and abscess) compartments (Li & Fishman, 2003). Risk factors include diabetes mellitus, obesity, current cigarette smoking, and steroid therapy. Surgical risk factors include complexity of surgery, type of bone saw used, type of sternal closure, length of surgical time, blood transfusions, and early reexploration to control hemorrhage. The CTA is important in revealing the extent and depth of infection, which, in turn, will help guide treatment planning. Usually, the preservation of mediastinal fat planes in CTA excludes surgical intervention. On the other hand, obliteration of mediastinal fat planes and diffuse soft tissue infiltration without or with gas collection, or low-density fluid collections within the mediastinum, are concerning for sternal infection. Recently published studies reported a 1-year mortality rate of approximately 22% (Loop et al., 1986; Sarr et al., 1984).

5.6 Pulmonary embolism

Clinical diagnosis of deep vein thrombosis and pulmonary embolism may be especially challenging because postoperative atelectasis, pleural effusion, or fluid overload may all contribute to the development of chest pain and dyspnea after CABG surgery. A recent report regarding pulmonary embolism in the post-CABG surgery population showed an overall prevalence of 23% for deep vein thrombosis by 1 week after surgery, with less than 2% of these cases identified clinically (Shammas, 2000).

5.7 Incidental findings

Although the intent of CTA after CABG surgery is to assess bypass graft patency and surgical complications, incidental findings are also frequently detected. In a recent study, 13.1% of patients in the immediate postoperative period had unsuspected noncardiac findings, including pulmonary embolism, pulmonary nodules, pneumonia, mucous plugging, and pneumothorax. (Mueller et al., 2007) Therefore, radiologists need to be aware of clinically significant findings with possible life-threatening consequences.

6. Conclusions

In recent years, MDCT with retrospective ECG gating has gained rapid acceptance as a diagnostic cardiac imaging modality, allowing assessment of coronary bypass graft patency with high spatial resolution. This tool could play an important role in patients with recurrence of chest pain or with unclear stress test results after myocardial revascularization surgery. Furthermore, the newest technological development of the CT scanner could strengthen the role of MDCT before percutaneous intervention of occluded or stenotic grafts, allowing the consensual assessment of occluded or stenotic bypass grafts which are difficult or impossible to be visualized with invasive coronary angiography. Therefore, it is crucial that cardiologists and radiologists understand CABG anatomy with knowledge of the type and number of bypass grafts used during myocardial revascularization surgery.

7. Reference

Achenbach, S.; Moshage, W.; Ropers, D.; Nossen, J. & Bachmann, K. (1997). Noninvasive, three-dimensional visualization of coronary artery bypass grafts by electron beam tomography. *American Journal of Cardiology*, Vol.79, No.7, (Apr 1 1997), pp. 856-861, ISSN 0002-9149

Anders, K.; Baum, U.; Schmid, M.; Ropers, D.; Schmid, A.; Pohle, K.; Daniel, W. G.; Bautz, W. & Achenbach, S. (2006). Coronary artery bypass graft (CABG) patency: assessment with high-resolution submillimeter 16-slice multidetector-row computed tomography (MDCT) versus coronary angiography. *European Journal of Radiology*, Vol.57, No.3, (Mar 2006), pp. 336-344, ISSN 0720-048X

Bourassa, M. G.; Fisher, L. D.; Campeau, L.; Gillespie, M. J.; McConney, M. & Lesperance, J. (1985). Long-term fate of bypass grafts: the Coronary Artery Surgery Study (CASS) and Montreal Heart Institute experiences. *Circulation*, Vol.72, No.6 Pt 2, (Dec 1985), pp. V71-78, ISSN 0009-7322

Buche, M.; Schoevaerdts, J. C.; Louagie, Y.; Schroeder, E.; Marchandise, B.; Chenu, P.; Dion, R.; Verhelst, R.; Deloos, M.; Gonzales, E. & et al. (1992). Use of the inferior epigastric artery for coronary bypass. *Journal of Thoracic and Cardiovascular Surgery*, Vol.103, No.4, (Apr 1992), pp. 665-670, ISSN 0022-5223

Campeau, L.; Enjalbert, M.; Lesperance, J.; Vaislic, C.; Grondin, C. M. & Bourassa, M. G. (1983). Atherosclerosis and late closure of aortocoronary saphenous vein grafts: sequential angiographic studies at 2 weeks, 1 year, 5 to 7 years, and 10 to 12 years after surgery. *Circulation*, Vol.68, No.3 Pt 2, (Sep 1983), pp. II1-7, ISSN 0009-7322

Carpentier, A.; Guermonprez, J. L.; Deloche, A.; Frechette, C. & DuBost, C. (1973). The aorta-to-coronary radial artery bypass graft. A technique avoiding pathological changes in grafts. *Annals of Thoracic Surgery*, Vol.16, No.2, (Aug 1973), pp. 111-121, ISSN 0003-4975

Carrel, T. P.; Eckstein, F. S.; Englberger, L.; Windecker, S. & Meier, B. (2003). Pitfalls and key lessons with the symmetry proximal anastomotic device in coronary artery bypass surgery. *Annals of Thoracic Surgery*, Vol.75, No.5, (May 2003), pp. 1434-1436, ISSN 0003-4975

Dikkers, R.; Willems, T. P.; Tio, R. A.; Anthonio, R. L.; Zijlstra, F. & Oudkerk, M. (2007). The benefit of 64-MDCT prior to invasive coronary angiography in symptomatic post-CABG patients. *International Journal of Cardiovascular Imaging*, Vol.23, No.3, (Jun 2007), pp. 369-377, ISSN 1569-5794

Dubois, C. L. & Vandervoort, P. M. (2001). Aneurysms and pseudoaneurysms of coronary arteries and saphenous vein coronary artery bypass grafts: a case report and literature review. Acta Cardiologica, Vol.56, No.4, (Aug 2001), pp. 263-267, ISSN 0001-5385

Engelmann, M. G.; von Smekal, A.; Knez, A.; Kurzinger, E.; Huehns, T. Y.; Hofling, B. & Reiser, M. (1997). Accuracy of spiral computed tomography for identifying arterial and venous coronary graft patency. *American Journal of Cardiology*, Vol.80, No.5, (Sep 1 1997), pp. 569-574, ISSN 0002-9149

Fitzgibbon, G. M.; Kafka, H. P.; Leach, A. J.; Keon, W. J.; Hooper, G. D. & Burton, J. R. (1996). Coronary bypass graft fate and patient outcome: angiographic follow-up of 5,065 grafts related to survival and reoperation in 1,388 patients during 25 years. *Journal*

of the American College of Cardiology, Vol.28, No.3, (Sep 1996), pp. 616-626, ISSN 0735-1097

Frazier, A. A.; Qureshi, F.; Read, K. M.; Gilkeson, R. C.; Poston, R. S. & White, C. S. (2005). Coronary artery bypass grafts: assessment with multidetector CT in the early and late postoperative settings. *Radiographics*, Vol.25, No.4, (Jul-Aug 2005), pp. 881-896, ISSN 1527-1323

Fullerton, D. A.; St Cyr, J. A.; Fall, S. M. & Whitman, G. J. (1994). Protection of the patent internal mammary artery by-pass graft from subsequent sternotomy. *Journal of Cardiovascular Surgery*, Vol.35, No.6, (Dec), pp. 499-501, ISSN 0021-9509

Gilkeson, R. C.; Markowitz, A. H. & Ciancibello, L. (2003). Multisection CT evaluation of the reoperative cardiac surgery patient. *Radiographics*, Vol.23 Spec No, (Oct 2003), pp. S3-17, ISSN 1527-1323

Gillinov, A. M.; Casselman, F. P.; Lytle, B. W.; Blackstone, E. H.; Parsons, E. M.; Loop, F. D. & Cosgrove, D. M., 3rd (1999). Injury to a patent left internal thoracic artery graft at coronary reoperation. *Annals of Thoracic Surgery*, Vol.67, No.2, (Feb 1999), pp. 382-386, ISSN 0003-4975

Hecht, H. S. & Roubin, G. (2007). Usefulness of computed tomographic angiography guided percutaneous coronary intervention. *American Journal of Cardiology*, Vol.99, No.6, (Mar 15 2007), pp. 871-875, ISSN 0002-9149

Hurlbut, D.; Myers, M. L.; Lefcoe, M. & Goldbach, M. (1990). Pleuropulmonary morbidity: internal thoracic artery versus saphenous vein graft. *Annals of Thoracic Surgery*, Vol.50, No.6, (Dec 1990), pp. 959-964, ISSN 0003-4975

Katara, A. N.; Samra, S. S. & Bhandarkar, D. S. (2003). Thoracoscopic window for a post-coronary artery bypass grafting pericardial effusion. *Indian Heart Journal*, Vol.55, No.2, (Mar-Apr 2003), pp. 180-181, ISSN 0019-4832

Kuvin, J. T.; Harati, N. A.; Pandian, N. G.; Bojar, R. M. & Khabbaz, K. R. (2002). Postoperative cardiac tamponade in the modern surgical era. *Annals of Thoracic Surgery*, Vol.74, No.4, (Oct 2002), pp. 1148-1153, ISSN 0003-4975

Lee, R.; Lim, J.; Kaw, G.; Wan, G.; Ng, K. & Ho, K. T. (2010). Comprehensive noninvasive evaluation of bypass grafts and native coronary arteries in patients after coronary bypass surgery: accuracy of 64-slice multidetector computed tomography compared to invasive coronary angiography. *Journal of Cardiovascular Medicine (Hagerstown)*, Vol.11, No.2, (Feb 2010), pp. 81-90, ISSN 1558-2035

Li, A. E. & Fishman, E. K. (2003). Evaluation of complications after sternotomy using single- and multidetector CT with three-dimensional volume rendering. *AJR. American Journal of Roentgenology*, Vol.181, No.4, (Oct 2003), pp. 1065-1070, ISSN 0361-803X

Locker, C.; Mohr, R.; Paz, Y.; Lev-Ran, O.; Herz, I.; Uretzky, G. & Shapira, I. (2002). Pretreatment with alpha-adrenergic blockers for prevention of radial artery spasm. *Annals of Thoracic Surgery*, Vol.74, No.4, (Oct 2002), pp. S1368-1370, ISSN 0003-4975

Loop, F. D.; Lytle, B. W.; Cosgrove, D. M.; Stewart, R. W.; Goormastic, M.; Williams, G. W.; Golding, L. A.; Gill, C. C.; Taylor, P. C.; Sheldon, W. C. & et al. (1986). Influence of the internal-mammary-artery graft on 10-year survival and other cardiac events. *New England Journal of Medicine*, Vol.314, No.1, (Jan 1986), pp. 1-6, ISSN 0028-4793

Mack, M. J.; Emery, R. W.; Ley, L. R.; Cole, P. A.; Leonard, A.; Edgerton, J. R.; Dewey, T. M.; Magee, M. J. & Flavin, T. S. (2003). Initial experience with proximal anastomoses

performed with a mechanical connector. *Annals of Thoracic Surgery*, Vol.75, No.6, (Jun 2003), pp. 1866-1870; discussion 1870-1871, ISSN 0003-4975

Manapat, A. E.; McCarthy, P. M.; Lytle, B. W.; Taylor, P. C.; Loop, F. D.; Stewart, R. W.; Rosenkranz, E. R.; Sapp, S. K.; Miller, D. & Cosgrove, D. M. (1994). Gastroepiploic and inferior epigastric arteries for coronary artery bypass. Early results and evolving applications. *Circulation*, Vol.90, No.5 Pt 2, (Nov 1994), pp. II144-147, ISSN 0009-7322

Marano, R.; Storto, M. L.; Maddestra, N. & Bonomo, L. (2004). Non-invasive assessment of coronary artery bypass graft with retrospectively ECG-gated four-row multi-detector spiral computed tomography. *European Radiology*, Vol.14, No.8, (Aug 2004), pp. 1353-1362, ISSN 0938-7994

Marano, R.; Storto, M. L.; Merlino, B.; Maddestra, N.; Di Giammarco, G. & Bonomo, L. (2005). A pictorial review of coronary artery bypass grafts at multidetector row CT. *Chest*, Vol.127, No.4, (Apr 2005), pp. 1371-1377, ISSN 0012-3692

Memon, A. Q.; Huang, R. I.; Marcus, F.; Xavier, L. & Alpert, J. (2003). Saphenous vein graft aneurysm: case report and review. *Cardiology in Review*, Vol.11, No.1, (Jan-Feb 2003), pp. 26-34, ISSN 1061-5377

Meurin, P.; Weber, H.; Renaud, N.; Larrazet, F.; Tabet, J. Y.; Demolis, P. & Ben Driss, A. (2004). Evolution of the postoperative pericardial effusion after day 15: the problem of the late tamponade. *Chest*, Vol.125, No.6, (Jun 2004), pp. 2182-2187, ISSN 0012-3692

Mohara, J.; Konishi, H.; Kato, M.; Misawa, Y.; Kamisawa, O. & Fuse, K. (1998). Saphenous vein graft pseudoaneurysm rupture after coronary artery bypass grafting. *Annals of Thoracic Surgery*, Vol.65, No.3, (Mar 1998), pp. 831-832, ISSN 0003-4975

Motwani, J. G. & Topol, E. J. (1998). Aortocoronary saphenous vein graft disease: pathogenesis, predisposition, and prevention. *Circulation*, Vol.97, No.9, (Mar 10 1998), pp. 916-931, ISSN 0009-7322

Mueller, J.; Jeudy, J.; Poston, R. & White, C. S. (2007). Cardiac CT angiography after coronary bypass surgery: prevalence of incidental findings. *AJR. American Journal of Roentgenology*, Vol.189, No.2, (Aug 2007), pp. 414-419, ISSN 1546-3141

Muneretto, C.; Bisleri, G.; Negri, A.; Manfredi, J.; Metra, M.; Nodari, S.; Culot, L. & Dei Cas, L. (2003). Total arterial myocardial revascularization with composite grafts improves results of coronary surgery in elderly: a prospective randomized comparison with conventional coronary artery bypass surgery. *Circulation*, Vol.108 Suppl 1, (Sep 2003), pp. II29-33, ISSN 1524-4539

Myers, M. G. & Fremes, S. E. (2003). Prevention of radial artery graft spasm: a survey of Canadian surgical centres. *Canadian Journal of Cardiology*, Vol.19, No.6, (May 2003), pp. 677-681, ISSN 0828-282X

Ohtsuka, T.; Akahane, M.; Ohtomo, K.; Kotsuka, Y. & Takamoto, S. (2000). Three-dimensional computed tomography for reoperative minimally invasive coronary artery bypass. *Annals of Thoracic Surgery*, Vol.70, No.5, (Nov 2000), pp. 1734-1735, ISSN 0003-4975

Peng, M. J.; Vargas, F. S.; Cukier, A.; Terra-Filho, M.; Teixeira, L. R. & Light, R. W. (1992). Postoperative pleural changes after coronary revascularization. Comparison between saphenous vein and internal mammary artery grafting. *Chest*, Vol.101, No.2, (Feb 1992), pp. 327-330, ISSN 0012-3692

Pepi, M.; Muratori, M.; Barbier, P.; Doria, E.; Arena, V.; Berti, M.; Celeste, F.; Guazzi, M. & Tamborini, G. (1994). Pericardial effusion after cardiac surgery: incidence, site, size, and haemodynamic consequences. *British Heart Journal*, Vol.72, No.4, (Oct 1994), pp. 327-331, ISSN 0007-0769

Possati, G.; Gaudino, M.; Prati, F.; Alessandrini, F.; Trani, C.; Glieca, F.; Mazzari, M. A.; Luciani, N. & Schiavoni, G. (2003). Long-term results of the radial artery used for myocardial revascularization. *Circulation*, Vol.108, No.11, (Sep 2003), pp. 1350-1354, ISSN 1524-4539

Poston, R.; White, C.; Read, K.; Gu, J.; Lee, A.; Avari, T. & Griffith, B. (2004). Virchow triad, but not use of an aortic connector device, predicts early graft failure after off-pump coronary bypass. *Heart Surg Forum*, Vol.7, No.5, pp. E428-433, ISSN 1522-6662

Pym, J.; Brown, P. M.; Charrette, E. J.; Parker, J. O. & West, R. O. (1987). Gastroepiploic-coronary anastomosis. A viable alternative bypass graft. *Journal of Thoracic and Cardiovascular Surgery*, Vol.94, No.2, (Aug 1987), pp. 256-259, ISSN 0022-5223

Ricci, M.; Karamanoukian, H. L.; D'Ancona, G.; Salerno, T. A. & Bergsland, J. (2000). Reoperative "off-pump" circumflex revascularization via left thoracotomy: how to prevent graft kinking. *Annals of Thoracic Surgery*, Vol.70, No.1, (Jul 2000), pp. 309-310, ISSN 0003-4975

Ropers, D.; Pohle, F. K.; Kuettner, A.; Pflederer, T.; Anders, K.; Daniel, W. G.; Bautz, W.; Baum, U. & Achenbach, S. (2006). Diagnostic accuracy of noninvasive coronary angiography in patients after bypass surgery using 64-slice spiral computed tomography with 330-ms gantry rotation. *Circulation*, Vol.114, No.22, (Nov 2006), pp. 2334-2341; quiz 2334, ISSN 1524-4539

Ropers, D.; Ulzheimer, S.; Wenkel, E.; Baum, U.; Giesler, T.; Derlien, H.; Moshage, W.; Bautz, W. A.; Daniel, W. G.; Kalender, W. A. & Achenbach, S. (2001). Investigation of aortocoronary artery bypass grafts by multislice spiral computed tomography with electrocardiographic-gated image reconstruction. *American Journal of Cardiology*, Vol.88, No.7, (Oct 2001), pp. 792-795, ISSN 0002-9149

Roy, M. C. (1998). Surgical-site infections after coronary artery bypass graft surgery: discriminating site-specific risk factors to improve prevention efforts. *Infection Control and Hospital Epidemiology*, Vol.19, No.4, (Apr 1998), pp. 229-233, ISSN 0899-823X

Sarr, M. G.; Gott, V. L. & Townsend, T. R. (1984). Mediastinal infection after cardiac surgery. *Annals of Thoracic Surgery*, Vol.38, No.4, (Oct 1984), pp. 415-423, ISSN 0003-4975

Schlosser, T.; Konorza, T.; Hunold, P.; Kuhl, H.; Schmermund, A. & Barkhausen, J. (2004). Noninvasive visualization of coronary artery bypass grafts using 16-detector row computed tomography. *Journal of the American College of Cardiology*, Vol.44, No.6, (Sep 2004), pp. 1224-1229, ISSN 0735-1097

Seifarth, H.; Raupach, R.; Schaller, S.; Fallenberg, E. M.; Flohr, T.; Heindel, W.; Fischbach, R. & Maintz, D. (2005). Assessment of coronary artery stents using 16-slice MDCT angiography: evaluation of a dedicated reconstruction kernel and a noise reduction filter. *European Radiology*, Vol.15, No.4, (Apr 2005), pp. 721-726, ISSN 0938-7994

Shammas, N. W. (2000). Pulmonary embolus after coronary artery bypass surgery: a review of the literature. *Clinical Cardiology*, Vol.23, No.9, (Sep 2000), pp. 637-644, ISSN 0160-9289

Song, B. G.; Choi, J. H.; Choi, S. M.; Park, J. H.; Park, Y. H. & Choe, Y. H. (2010). Coronary artery graft dilatation aided by multidetector computed tomography. *Asian Cardiovascular and Thoracic Annals*, Vol.18, No.2, (Feb 2010), pp. 177-179, ISSN 1816-5370

Tochii, M.; Takagi, Y.; Anno, H.; Hoshino, R.; Akita, K.; Kondo, H. & Ando, M. (2010). Accuracy of 64-slice multidetector computed tomography for diseased coronary artery graft detection. *Annals of Thoracic Surgery*, Vol.89, No.6, (Jun 2010), pp. 1906-1911, ISSN 1552-6259

Traverse, J. H.; Mooney, M. R.; Pedersen, W. R.; Madison, J. D.; Flavin, T. F.; Kshettry, V. R.; Henry, T. D.; Eales, F.; Joyce, L. D. & Emery, R. W. (2003). Clinical, angiographic, and interventional follow-up of patients with aortic-saphenous vein graft connectors. *Circulation*, Vol.108, No.4, (Jul 2003), pp. 452-456, ISSN 1524-4539

Ueyama, K.; Ohashi, H.; Tsutsumi, Y.; Kawai, T.; Ueda, T. & Ohnaka, M. (1999). Evaluation of coronary artery bypass grafts using helical scan computed tomography. *Catheterization and Cardiovascular Interventions*, Vol.46, No.3, (Mar 1999), pp. 322-326, ISSN 1522-1946

Vargas, F. S.; Cukier, A.; Hueb, W.; Teixeira, L. R. & Light, R. W. (1994). Relationship between pleural effusion and pericardial involvement after myocardial revascularization. *Chest*, Vol.105, No.6, (Jun 1994), pp. 1748-1752, ISSN 0012-3692

Vembar, M.; Garcia, M. J.; Heuscher, D. J.; Haberl, R.; Matthews, D.; Bohme, G. E. & Greenberg, N. L. (2003). A dynamic approach to identifying desired physiological phases for cardiac imaging using multislice spiral CT. *Medical Physics*, Vol.30, No.7, (Jul 2003), pp. 1683-1693, ISSN 0094-2405

Wiklund, L.; Bugge, M. & Berglin, E. (2002). Angiographic results after the use of a sutureless aortic connector for proximal vein graft anastomoses. *Annals of Thoracic Surgery*, Vol.73, No.6, (Jun 2002), pp. 1993-1994, ISSN 0003-4975

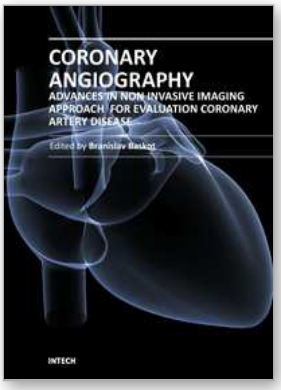

Coronary Angiography - Advances in Noninvasive Imaging Approach for Evaluation of Coronary Artery Disease

Edited by Prof. Baskot Branislav

ISBN 978-953-307-675-1
Hard cover, 414 pages
Publisher InTech
Published online 15, September, 2011
Published in print edition September, 2011

In the intervening 10 years tremendous advances in the field of cardiac computed tomography have occurred. We now can legitimately claim that computed tomography angiography (CTA) of the coronary arteries is available. In the evaluation of patients with suspected coronary artery disease (CAD), many guidelines today consider CTA an alternative to stress testing. The use of CTA in primary prevention patients is more controversial in considering diagnostic test interpretation in populations with a low prevalence to disease. However the nuclear technique most frequently used by cardiologists is myocardial perfusion imaging (MPI). The combination of a nuclear camera with CTA allows for the attainment of coronary anatomic, cardiac function and MPI from one piece of equipment. PET/SPECT cameras can now assess perfusion, function, and metabolism. Assessing cardiac viability is now fairly routine with these enhancements to cardiac imaging. This issue is full of important information that every cardiologist needs to now.

INTECH
open science | open minds

InTech Europe
University Campus STeP Ri
Slavka Krautzeka 83/A
51000 Rijeka, Croatia
Phone: +385 (51) 770 447
Fax: +385 (51) 686 166
www.intechopen.com

InTech China
Unit 405, Office Block, Hotel Equatorial Shanghai
No.65, Yan An Road (West), Shanghai, 200040, China
中国上海市延安西路65号上海国际贵都大饭店办公楼405单元
Phone: +86-21-62489820
Fax: +86-21-62489821